REVIEW

In vivo magnetic resonance spectroscopy: basic methodology and clinical applications

Marinette van der Graaf

Abstract The clinical use of in vivo magnetic resonance spectroscopy (MRS) has been limited for a long time, mainly due to its low sensitivity. However, with the advent of clinical MR systems with higher magnetic field strengths such as 3 Tesla, the development of better coils, and the design of optimized radio-frequency pulses, sensitivity has been considerably improved. Therefore, in vivo MRS has become a technique that is routinely used more and more in the clinic. In this review, the basic methodology of in vivo MRS is described—mainly focused on ^{1}H MRS of the brain—with attention to hardware requirements, patient safety, acquisition methods, data post-processing, and quantification. Furthermore, examples of clinical applications of in vivo brain MRS in two interesting fields are described. First, together with a description of the major resonances present in brain MR spectra, several examples are presented of deviations from the normal spectral pattern associated with inborn errors of metabolism. Second, through examples of MR spectra of brain tumors, it is shown that MRS can play an important role in oncology.

The more you see: spectroscopy in molecular biophysics.

M. van der Graaf (✉)
Clinical Physics Laboratory, Department of Paediatrics 833,
Radboud University Nijmegen Medical Centre, P.O. Box 9101,
6500 HB Nijmegen, The Netherlands
e-mail: M.vanderGraaf@rad.umcn.nl

M. van der Graaf
Department of Radiology, Radboud University Nijmegen
Medical Centre, Nijmegen, The Netherlands

Abbreviations

1D, 2D, 3D	One-, two-, three-dimensional
Acq	Acquisition
Ala	Alanine
CHESS	Chemical shift—selective water suppression
Cho	Choline
Cre	Creatine
CSD	Chemical shift displacement
CSI	Chemical shift imaging
ECC	Eddy current correction
FOV	Field of view
FT	Fourier transformation
GABA	γ-Aminobutyric acid
Gln	Glutamine
Glu	Glutamate
Glx	Glutamine + glutamate
Gly	Glycine
Ins	Myo-inositol
jMRUI	Java-based magnetic resonance user interface
Lac	Lactate
Lip	Lipid
LCModel	Linear combination of model spectra
MM	Macromolecules
MR	Magnetic resonance
MRI	Magnetic resonance imaging
MRS	Magnetic resonance spectroscopy
MRSI	Magnetic resonance spectroscopic imaging
NAA	N-acetyl aspartate
NAAG	N-acetylaspartyl glutamate

NMR	Nuclear magnetic resonance
PRESS	Point-resolved spectroscopy
RF	Radio frequency
SAR	Specific absorption rate
SNR	Signal-to-noise ratio
STEAM	Stimulated echo acquisition mode
SVS	Single voxel spectroscopy
Tau	Time delay in PRESS
T	Tesla
TE	Echo time
TM	Mixing time
TR	Repetition time
VOI	Volume of interest
WET	Water suppression enhanced through T1 effects

Introduction

Nuclear magnetic resonance (NMR) spectroscopy is generally known as an analytical method in chemistry to identify molecules and to determine their biophysical characteristics. The main application of nuclear magnetic resonance in the clinic is, without a doubt, to obtain detailed anatomical images non-invasively throughout the human body by magnetic resonance imaging (MRI). However, not only MRI but also NMR spectroscopy has several clinical and biomedical applications. When an NMR technique is used in vivo and in particular in the clinic, the convention is to leave the term "nuclear" out of the name as inclusion of this part may erroneously lead to associations with nuclear medicine, radioactive materials, and ionizing radiation. Therefore, in vivo NMR spectroscopy is referred to as magnetic resonance spectroscopy (MRS). Just as in its application in chemistry, MRS allows the detection of relatively small molecules, typically in concentrations of 0.5–10 mM, with sufficiently high flexibility within cells or in extra-cellular spaces. The obtained MR spectra supply information on metabolic pathways and changes therein, which makes MRS a very suitable technique to monitor metabolic changes due to disease and to follow treatment. In this review an overview is presented on in vivo MRS methodology and some biomedical and clinical applications, by which persons familiar with the chemical application of NMR spectroscopy may learn about its application in the clinic. Most emphasis is laid on ^{1}H MRS of the human brain, which is the main clinical MRS application. As it is impossible to give a complete description of all biomedical applications of in vivo MRS, this review is limited to examples of human brain MRS in the identification of inborn errors

in metabolism, and diagnostics and research in brain cancer.

In vivo MRS methodology

Basic requirements

MR spectra can be obtained of several metabolites in the human body by using various nuclei, such as ^{1}H, ^{31}P, ^{19}F, ^{13}C, ^{23}Na, which all can provide valuable metabolic and physiological information. In biomedicine, however, mainly ^{1}H MRS is used because of the high sensitivity of the ^{1}H nucleus, the almost 100% availability of this isotope, and the abundant presence of this nucleus in most metabolites. In addition, ^{1}H MRS can be performed relatively easily using clinical MR imaging systems with standard radio-frequency (RF) coils developed for the acquisition of diagnostic MR images. In fact, the MR signal of the ^{1}H nuclei in water and fat is used to obtain MR images. Common clinical MR systems have magnetic field strengths between 0.2 and 3 Tesla (T). In MRS applications, it is generally not the signals of water and fat that are of interest, but rather the smaller metabolite signals, thus a magnetic field of sufficient strength is required. Therefore, most clinical MRS measurements are performed using MR systems with field strengths of 1.5 T or higher. In particular, the advent of clinical MR systems with a field strength of 3 T has improved signal-to-noise ratio (SNR) in MR spectra, creating the possibility of obtaining spectra from smaller volumes.

In the last few years, human MR systems with much higher field strengths of 7 and 9.4 T have been installed, and NeuroSpin in Saclay (France) even has plans for an 11.7 T MR system to become available for human applications in 2011. At the moment, however, such MR systems with ultra high fields are only used for scientific research and their clinical usefulness is still under debate because of very high costs, several technical challenges, and concerns about biological effects (Hennig 2008). In addition to the main magnet to create a strong static magnetic field (B_0), gradient coils are used to generate magnetic field gradients in three directions (G_x, G_y, and G_z); these are necessary for selection of the volume of interest (VOI) from which the MRS signal is obtained. These field gradients are in the range of 10–50 mT/m with a switching time on the order of a millisecond.

For ^{1}H MRS, the RF body coil built inside the magnet bore may be used as an RF transmitter in combination with another coil positioned on the surface or around the body for RF signal reception (Fig. 1). Another possibility is the use of a transmit-receive coil, which is used for both transmission and reception. In recent years, many

Fig. 1 Pediatric patient positioned in the headcoil on the table of the MR system just before the table with patient and coil is moved into the magnetic bore for the MR investigation

improvements in MR coil design have been made, for example the development of various phased-array coil designs, which has resulted in improved sensitivity (Fujita 2007). A small surface coil yields a higher SNR closer to the coil surface than a volume coil, but the sensitive region is much smaller. Through the combination of multiple surface coils in a phased-array coil concept, high SNR can be combined with an extended field of view (FOV). For MRS using nuclei other than ^{1}H, the standard MRI coils can not be used, but special coils tuned to the desired nucleus have to be bought or built. Often these coils consist of multiple coils, one tuned to the desired nucleus such as ^{31}P or ^{13}C and another tuned to ^{1}H to allow decoupling or polarization transfer.

For all MR examinations, both MRI and MRS, some safety precautions have to be taken against potential risks caused by the main magnetic field, the switching of the magnetic field gradients, or the RF radiation. No harmful physiological effects are known to be caused by the main magnetic field of clinical MR systems of 1.5–3 T, but the strong magnetic field does attract ferromagnetic objects. It should be determined if the patient has an implanted electronic device such as a pacemaker or an internal defibrillator or other magnetic material such as cochlear implants or ferromagnetic aneurysm clips. Also the presence of metal splinters at critical locations, e.g. in the eye or in the brain is a contra-indication for an MR investigation. And even a clinician entering the room with loose metal objects such as a pen or a pair of scissors in his pocket may become a danger for a patient lying in the magnet, as these objects can be launched in the direction of the patient by the strong magnetic field. In addition, watches and credit cards should be left outside the room as these may be damaged by the magnetic field.

The switching of the magnetic field gradients produces an acoustic noise for which the patients should wear ear protection. In addition, fast gradient switching may induce nerve stimulation, but such fast switching is not often applied in MRS, and on clinical scanners the gradients used are monitored and a warning appears if gradient switching becomes too fast. The final effect may be slight heating (<1–2°C) of the patient by RF radiation. The amount of energy absorbed per mass of tissue, defined as specific absorption rate (SAR), is also monitored and strictly limited on clinical MR systems. One contra-indication not related to safety is claustrophobia. Patients with severe claustrophobia and also patients who cannot lie down without movement such as young children may be sedated or anesthetized to undergo an MR investigation.

MRS data acquisition

Generally an MRS examination starts with the acquisition of some anatomical MR images of the organ of interest. Then, these MR images are used as a guide to select a volume of tissue from which the MR spectrum will be acquired. In single voxel spectroscopy (SVS), this can be a single volume positioned in a tumor or in a particular location where metabolism may be disturbed due to the disease of the patient. Another possibility is magnetic resonance spectroscopic imaging (MRSI), originally introduced as chemical shift imaging (CSI; Brown et al. 1982), in which a large volume is divided in multiple smaller voxels, with each giving rise to a spectrum simultaneously. This technique, a sort of hybrid of MRS and MRI, is suitable for the detection of spatial distributions, e.g., to determine the region affected by tumor infiltrations. In ^{1}H MRS, techniques such as chemical shift-selective water suppression (CHESS; Haase et al. 1985) or water suppression enhanced through T1 effects (WET; Ogg et al. 1994) are usually used to suppress the water signal when metabolite spectra are acquired. In addition, a spectrum without water suppression is obtained, which can be used for line-shape corrections and quantification.

The predominant SVS techniques used for acquisition of ^{1}H MR spectra, mostly applied to the brain, are known as point-resolved spectroscopy (PRESS; Ordidge et al. 1985; Bottomley 1987) and stimulated echo acquisition mode (STEAM; Frahm et al. 1989). The main difference between STEAM and PRESS is the acquisition of a stimulated echo obtained by three 90° pulses in STEAM and a second echo obtained by a 90° excitation pulse followed by two 180° refocusing pulses in PRESS (see Fig. 2). In both methods, each of the three pulses is combined with a gradient in X, Y, or Z direction used to select a slice in that direction. Only the signal of the rectangular volume (single voxel) in which all three slices overlap is refocused and acquired. By
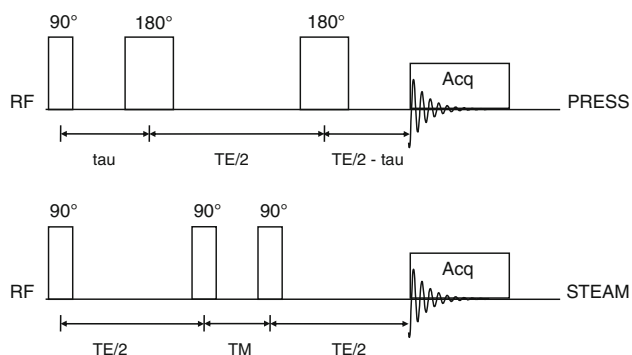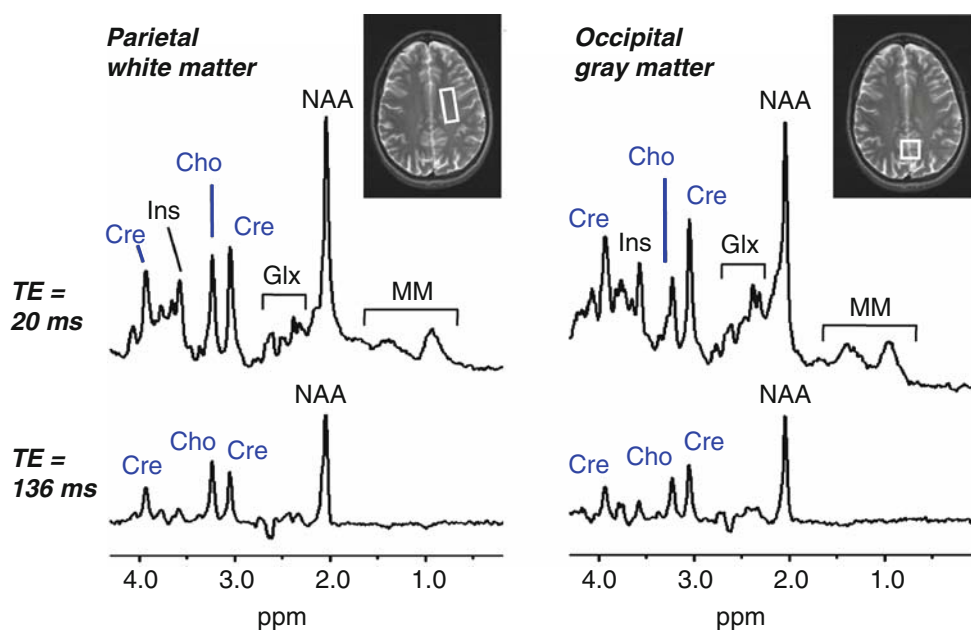
Fig. 2 Schematic overview of the pulse sequences PRESS and STEAM. It should be noted that each of the three RF pulses is combined with a gradient in three different directions (*X*, *Y*, and *Z*) to allow selection of a rectangular volume. *RF* Radio frequency, *tau* time delay between 90° and 180° pulses in PRESS, *TE* echo time, *TM* mixing time

changing the delay times between the pulses, the echo time (TE) can be altered. When a longer TE is used, the signal will be decreased due to T2 relaxation, and the phase of multiplet signals is changed due to J-coupling. For quantitative measurements, the combination of a short echo time and a long repetition time (TR) is generally used to obtain signals with minimal signal loss due to T2- and T1-weighting (Fig. 3, upper row). Longer TE measurements are used to obtain spectra with only a limited number of sharp (often singlet) resonances, which are relatively easy to analyze (Fig. 3, bottom row). Often a TE of 135–144 ms is used, as this results in a spectrum in which the doublet signal of lactate with a J-coupling constant of approximately 7 Hz is completely inverted (see Fig. 6 below).

An important difference between the two SVS pulse sequences is that, by acquisition of a stimulated echo in STEAM, half of the signal is not used resulting in a 50% lower SNR compared with PRESS. The disadvantage of PRESS volume selection has long been the use of two 180° pulses. As the maximum pulse intensity is limited, the pulse length of a 180° pulse is generally longer than the 90° pulse or the shape of the pulse is adapted to limit its length. Therefore, the presence of these two 180° pulses does not allow very short TE, they result in a less optimal slice selection profile, and their bandwidth is smaller, giving rise to a larger chemical shift displacement (CSD) artifact. This CSD artifact arises from the fact that signals with different chemical shifts experience different (frequency-encoded) slice selections and thus do not originate from exactly the same volume. This effect becomes larger at higher magnetic field strengths. For these reasons, STEAM is the method of choice for data acquisition with short TE and precise volume selection. Lately, however, the characteristics of the 180° pulses used in PRESS have been more and more improved, e.g. by numerical optimization (Schulte et al. 2008) or replacement of each 180° pulse by two adiabatic pulses (Scheenen et al. 2008). These developments, together with the very important factor of a doubled SNR compared with STEAM, have made the PRESS sequence the most popular SVS sequence for ^{1}H MRS currently.

In MRSI, phase-encoding gradients are used in one, two, or three dimensions (1D, 2D, 3D) to sample k-space (Skoch et al. 2008) for volume selection in a similar way as in MRI, but with larger volume elements (voxels). Generally these phase-encoding gradients are applied after

Fig. 3 Single-voxel MR spectra obtained at a field strength of 3T from white matter (*left*) and gray matter (*right*) from a healthy volunteer. The voxel positions are indicated in the corresponding MR images. Spectra were obtained with PRESS volume selection (TE/TR = 20/5,000 ms for *upper row* and TE/TR = 136/2,000 ms for *lower row*). The most prominent signals are labeled: *Cre* creatine, *Ins* myo-inositol, *Cho* choline, *Glx* glutamine and glutamate, *NAA* N-acetyl aspartate, *MM* macromolecules. Note the difference in relative signal intensities of Cho and Cre in white and gray matter, for which the labels are indicated in *blue*

Fig. 4a–d Magnetic resonance spectroscopic imaging (MRSI) data obtained from a patient with a brain tumor (low-grade oligodendroglioma). **a** MR image with volume of interest selected by STEAM in *white* and two-dimensional MRSI grid in *blue*. Spectra are only acquired from the MRSI voxels inside the volume of interest. The *dotted line* in **a** indicates the MRSI voxels shown in **b**. **b** Part of the spectral image showing MRSI voxels with their corresponding spectra. **c** Enlargement of the spectrum obtained from the voxel indicated in *red* in **b** and **c**. The spectrum (TE = 20 ms) shows a typical pattern for a low-grade brain tumor with increased choline, decreased NAA, and the doublet of lactate. **d** Metabolite map showing the intensity distribution of the ratio of choline to NAA over the volume of interest with the highest intensity indicated in *red* at the position of the tumor
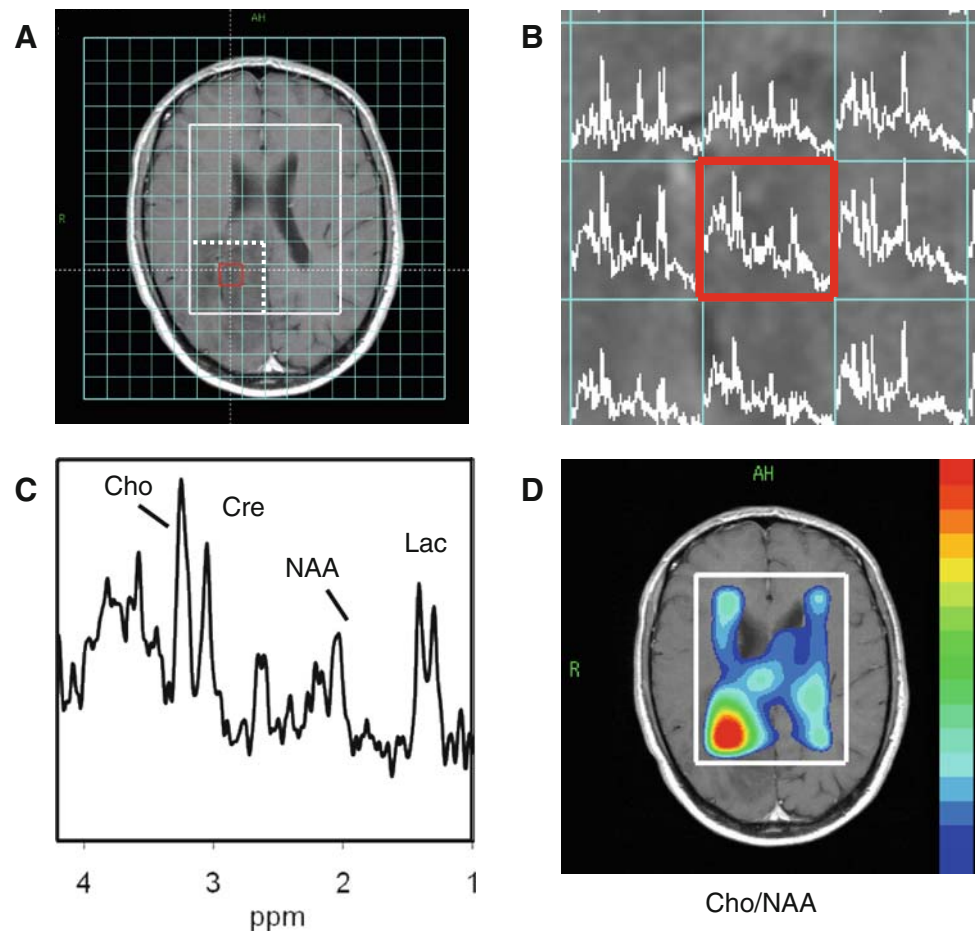
an excitation pulse in combination with a gradient for slice selection or with volume pre-selection in which a volume of interest selected by STEAM or PRESS is further subdivided into smaller voxels. In MRSI, spectra of all voxels are acquired simultaneously, and spatial distributions of various metabolites can be obtained in a single experiment (see Fig. 4). In contrary to the fixed voxel position in SVS, voxels obtained by phase encoding can be repositioned during post processing by grid shifting. The time needed to perform a classical MRSI experiment is at least equal to the number of phase-encoding steps multiplied by the TR. This means that the acquisition time is not larger than it is for SVS if the number of phase-encoding steps is equal to the number of averages required to obtain sufficient SNR. However, for signals with high intensity, the number of steps needed for spatial encoding in classical MRSI may be larger than the number of averages required for an acceptable SNR. To solve this time problem, only the phase-encoding steps that lead to sampling of the most important points in k-space inside the central circle (2D) or sphere (3D) can be used (Maudsley et al. 1994). Another possibility is to acquire multiple echoes with each echo encoding for a

different point in k-space in so-called turbo spectroscopic imaging (Duyn and Moonen 1993) or to use the delay TR to measure a data point for another slice in multislice MRSI (Duyn et al. 1993). More recently, other fast MRSI techniques have been developed in which varying gradient strengths during the data acquisition period are used for spatial encoding (Posse et al. 1994) or in which more recently developed parallel spectroscopic imaging techniques are implemented (Dydak et al. 2001). In particular, 3D applications of MRSI benefit from these accelerating modifications.

The main disadvantage of MRSI is the presence of so-called voxel bleed, which means that the spectrum of a voxel may be contaminated by signals originating from adjacent voxels with both positive and negative intensities due to the shape of the point spread function associated with the limited matrix size used in MRSI (Brown 1992). The effect of voxel bleed can be reduced by the use of special filters before Fourier transformation (FT) in the spatial domain, but this increases the dimensions of the voxels. Generally, SVS is used when accurate quantification is desirable, and MRSI is used to obtain information on spatial distributions.

Post-processing and quantification

Common post-processing of SVS spectra (in 't Zandt et al. 2001) includes multiplication with a filter in the time domain, zero-filling, FT, phasing, and baseline correction, which is basically not different from post-processing of high-resolution NMR data. In localized MRS, however, gradient switching may cause eddy current artifacts that are time and space dependent. Such artifacts in a metabolite spectrum can be removed with a reference water signal obtained without water suppression using the same sequence and from the same VOI. The method most commonly applied consists of a point-wise division in the time domain by the phase of the water signal at that particular time point (Klose 1990). This so-called eddy current correction (ECC) is applied as a first post-processing step, and it results in line-shape corrections in the metabolite spectrum together with the removal of offsets in zero-order phasing and frequency. Although eddy currents are smaller in modern MR systems making line-shape correction less essential, ECC correction is still commonly used for automatic phasing and frequency offset correction. In MRSI, the data are first multiplied with a filter (often Hamming or Hanning) followed by FT in the spatial domain. Thereafter, the time-domain data associated with each voxel are processed identically as SVS data to MR spectra. The spectra obtained from each voxel and their spatial origin can be shown in a spectral map (Fig. 4b). After the intensities of a certain metabolite signal in all spectra are quantified (see below), MRSI offers the possibility to construct a metabolite map in which the spatial distribution of the specific metabolite or a metabolite ratio is shown (Fig. 4d).

For quantification the integrals of the resonances present in the spectrum have to be determined. Presently two main approaches are followed using analyses in the frequency domain or in the time domain. Although on most MR systems, software programs are available to integrate the signals present in the MR spectrum or to fit them to model functions in order to obtain quantitative results, often software programs with more advanced algorithms are applied. A widely used software package for quantification is LCModel (linear combination of model spectra; Provencher 1993), in which frequency domain data are fitted to model spectra in a database resulting in intensity estimates of each metabolite. The model spectra in the database may be obtained from in vitro measurements of metabolite solutions using the same pulse sequence and timings as the in vivo measurement or by computer simulations. The advantage of the LCModel program is that the entire spectral pattern associated with each metabolite is used for the fitting. Therefore, the software package is very popular for the evaluation of ^{1}H MR spectra of the brain obtained

with a short TE, which show many—often overlapping—resonance lines (Fig. 3, upper row).

For spectra with fewer (overlapping) lines, such as ^{31}P MR spectra or ^{1}H MR spectra obtained with long TE (Fig. 3, lower row), the program jMRUI (Java-based magnetic resonance user interface; http://www.mrui.uab.es/mrui/) is generally used. In jMRUI, the data are fitted in the time domain using prior knowledge of frequencies, linewidths, coupling patterns, etc. By using time-domain fitting, uncertainties introduced by the shape of the baseline are avoided. In addition, the program offers the possibility to remove unwanted signals such as the water signal. Both software packages, LCModel and jMRUI, not only provide estimates on signal intensities but also give information on the quality of the fit with the Cramér-Rao lower bound as an error estimation (Cavassila et al. 2001).

The quantification methods described above result in signal intensities in arbitrary units, with ratios often used in clinical diagnosis. For brain spectra, the intensity of the methyl resonance of creatine is commonly used for normalization. Although this normalization removes differences, for example in volume and coil loading, a change in a ratio can be caused by changes in both numerator and denominator (Li et al. 2003). Therefore, for absolute quantification, referencing to an internal or external reference signal is necessary. The water signal obtained from the same volume is frequently used as an internal reference (e.g., Soher et al. 1996), but in this case a particular water content has to be assumed, which may be changed in pathology. When an external reference is used, the signals measured in vivo are correlated to the signal intensity of a compound with a known concentration in an external phantom, which can be present inside the coil at the time of the in vivo examination or which may be placed at the position of the patient afterwards. If a phantom replacement is used, the coil loading may be different from the situation in which the patient is measured, which affects signal intensity (Hoult and Richards 1976). For that reason, the signal intensity is corrected for coil loading differences using the reciprocity principle (Michaelis et al. 1993). For absolute quantification, it is best to acquire spectra with minimal T1- and T2-weighting by using a long TR and short TE, as each metabolite line has its own values for T1 and T2 relaxation, which makes it difficult to correct for relaxation effects.

The use of absolute quantification should in principle lead to metabolite tissue levels whose values can be compared among institutes, independent of the exact measurement method used. In practice, however, variations in data acquisition, post-processing, and quantification result in small differences, and metabolite values obtained from a patient can be best compared with a reference data set of "institutional units" obtained on healthy volunteers using

entirely identical procedures in the same institute. In this reference data set, the location of the VOI has to be taken into account, since the metabolic content and thus the spectrum deviate between gray and white matter in the brain (Fig. 3). And also the location within gray or white matter is of influence due to regional variations in metabolite concentrations; for instance the choline content of frontal gray matter is approximately 50% larger than that in occipital gray matter (Pouwels and Frahm 1998). Finally, patient age is important as metabolite concentration in the brain changes, both in children up to the age of ten years (Kreis et al. 1993; Pouwels et al. 1999) and in elderly people (Gruber et al. 2008).

Clinical applications

Normal brain and metabolic disorders

Estimations of the number of metabolites present in the human body range between 2,000 and 20,000 (Schmidt 2004). In patients with an inborn error in metabolism, the concentration of any of these metabolites may be unusually high or low due to an inherited defect in enzymatic activity. MRS is an ideal technique to measure changes in metabolite levels non-invasively, and thus the technique is very suitable in the diagnostics of metabolic disorders. However, it should be noted that only small metabolites with sufficiently high concentration can be observed by MRS. In addition, pattern changes in the MR spectrum may only be indicative of a general pathology such as demyelination in white matter or ischemia and not specific enough to identify a metabolic disorder. Still, such general pattern changes in combination with other clinical and biochemical information may help to find the correct diagnosis. In a recent review, Cecil showed brain ^{1}H MR spectra of many metabolic diseases, including lysosomal disorders, peroxisomal disorders, mitochondrial disorders, white-matter disorders, disorders of amino and organic acid metabolism, and some miscellaneous disorders (Cecil 2006). However, many of the spectra presented are not unique for the corresponding disease. Below, based upon the major resonances visible in the MR spectrum, examples are described in which the MR spectrum plays an important role in the identification of the disorder and the increase, decrease, presence, or absence of a resonance may be pathognomonic.

In ^{1}H MR spectra of the brain (Fig. 3), the most prominent signals are generally assigned as N-acetyl aspartate (NAA), creatine (Cre), and choline (Cho). In fact, each of these peaks arises from a number of compounds. The NAA signal at 2.01 ppm mainly originates from

the methyl group of N-acetyl aspartate but has some contribution of N-acetylaspartyl glutamate (NAAG; 2.04 ppm). The creatine peaks at 3.03 ppm (methyl protons) and 3.91 ppm (methylene protons) represent both creatine and phosphocreatine, and the choline resonance at 3.21 ppm contains signals from the three methyl groups of free choline (3.19 ppm), and in particular from the choline moieties present in glycerophosphoryl choline (3.21 ppm) and phosphocholine (3.21 ppm).

NAA is generally considered to be a neuronal marker, which is synthesized in the mitochondria of the neuron and transported along axons, but it has also been suggested to play a role as a cerebral osmolyte (Baslow 2002). The concentration of NAA is reduced in case of neuronal loss as in many white-matter diseases and also in brain tumors (see next section). One case of a child without NAA and NAAG in its brain MR spectrum has been reported (Martin et al. 2001); this complete absence is most likely due to a defect of the anabolic enzyme L-aspartate N-acetyltransferase. The opposite phenomenon—significant increase of the NAA resonance—is very specific for Canavan disease, which belongs to the group of neurotransmitter diseases (Fig. 5). Because of a deficiency in the enzyme aspartoacylase, NAA accumulates in the mitochondria and impairs myelin synthesis resulting in this severe white-matter disease (Janson et al. 2006). In Salla disease, the
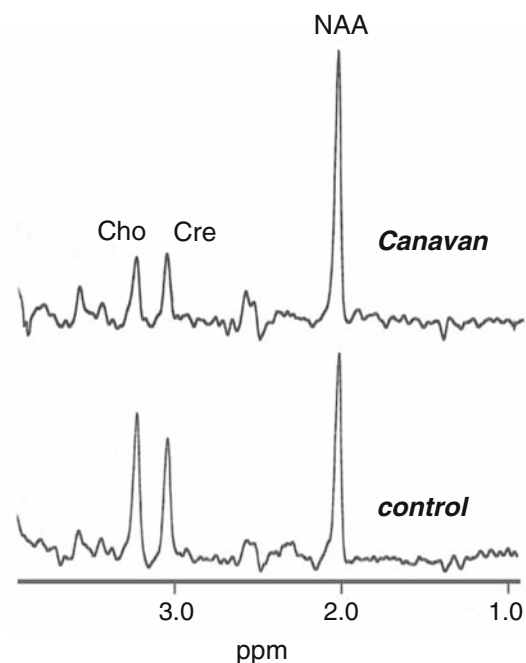

Fig. 5 MR spectra obtained at 1.5 T (TE/TR = 135/2,000 ms) of parietal white matter of a 13-month-old patient with Canavan disease (*upper row*) and an age-matched control (*lower row*). Note the remarkable increase in NAA signal in the spectrum of the patient, together with decreases in choline and creatine

NAA resonance may have a contribution of N-acetylneuraminic acid, but the increase in the NAA resonance is not so prominent, probably due to a concomitant decrease in N-acetyl aspartate (Varho et al. 1999).

Creatine and phosphocreatine are involved in energy metabolism, and their concentration is quite constant. Therefore, they are often used in the calculation of metabolite ratios. However, regional differences exist and also pathologies such as a tumor may reduce the Cre signal intensity. In contrast, gliosis in white matter may slightly increase the signal. Complete absence of the Cre signal points directly to a defect in creatine synthesis, as in guanidino acetate methyltransferase deficiency (Stöckler et al. 1994) or in L-arginine glycine amidinotransferase deficiency (Item et al. 2001), or to a creatine transporter defect (Cecil et al. 2001). It should be noted that a low Cre signal originating from food may occur in the brain of patients with a defect in Cre synthesis, although the increase in Cre concentration upon Cre supplementation is slow, and the concentration may still not be normalized after 2 years (Stöckler et al. 1996).

Choline and choline-containing compounds play an important role in membrane synthesis and an increase in the Cho signal is indicative of an increased membrane turnover. In tumors the choline signal is correlated with malignancy. However, in cerebral infarction and inflammation the Cho signal may also increase, which may hamper correct differentiation between tumors and other pathologies. No specific metabolic defects have been described so far in which the intensity of the choline peak may be decisive in the diagnosis.

In MR spectra obtained with short echo time, another prominent signal is visible at 3.6 ppm, which mainly originates from two protons of myo-inositol (Ins, 3.61 ppm) and also has a contribution of the singlet of glycine (Gly, 3.55 ppm). In particular in spectra obtained at a field strength of 1.5 T, the pseudo-singlet of Ins and the singlet of Gly are difficult to separate, but in spectra obtained at 3.0 T, the multiplet pattern of Ins is different and separation is feasible even at short echo time. Ins is a simple sugar that is primarily synthesized in glial cells and that is considered to be a glial marker and an osmolyte. The concentration of Ins increases with glial proliferation or with glial cell-size increase, both of which occur in inflammation. In addition, Ins may represent a breakdown product of myelin. Increased Ins is present in gliosis, astrocytosis, and in disorders such as Alzheimer disease, and its increase is not very specific. The signal of Gly present at almost the same chemical shift position has a longer transversal relaxation time, T2, so that it is also present in MR spectra obtained at longer echo times (e.g., 136 ms). Glycine is an amino acid, and a prominent increase in its concentration and its resonance peak has been observed in non-ketotic

hyperglycinemia originating from a defect in the glycine cleavage system (Heindel et al. 1993).

The doublet signal of the methyl group of lactate (Lac; center at 1.31 ppm), with its normal concentration of approximately 0.5 mM, is not or hardly visible in brain MR spectra. However, under anaerobic conditions its concentration increases and the lactate signal appears as a doublet with positive sign in spectra obtained with short echo times and as an inverted doublet in spectra obtained with a TE of 136 ms (see Fig. 6). Increased lactate signals occur when the normal aerobic oxidation mechanism fails and anaerobic glycolysis becomes more important, which may occur in many pathologies, such as hypoxia and ischemia, brain tumors, and metabolic defects, in particular mitochondrial disorders. In the brain of patients with a mitochondrial disorder, an increase in lactate signal can often be observed, in particular in spectra obtained from the basal ganglia (Fig. 6). The signal of the methyl group of the amino acid Alanine (Ala; center at 1.47 ppm) behaves similarly to the signal of Lac, with a positive sign at short TE and an inverted doublet at a TE of 136 ms. Ala can—just as Lac—be formed from pyruvate when the normal route of pyruvate into the Krebs cycle is disturbed. Increased levels of Ala can be found in defects in oxidative
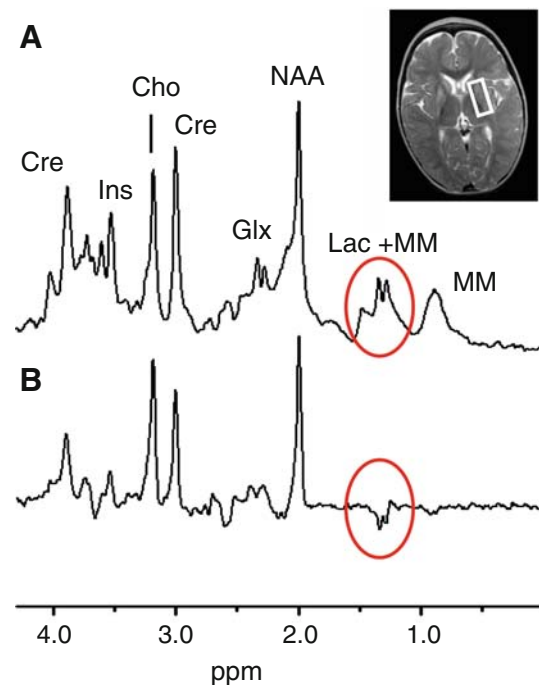

Fig. 6a, b MR spectra obtained at 3T of basal ganglia (voxel indicated on MR image) of a patient with Leigh syndrome, a mitochondrial disorder. Spectra were obtained with PRESS volume selection (TE/TR = 20/5,000 ms for **a** and TE/TR = 136/2,000 ms for **b**). In **a** increased lactate is present as a positive doublet at 1.3 ppm on top of the broad signal of macromolecules. In spectrum **b**, obtained with a longer TE of 136 ms, the broad signal of macromolecules is not present, and the lactate doublet is inverted

metabolism, and in tumors it is specific for meningiomas (Yue et al. 2008).

The last resonances that may appear with relatively high intensity in a brain proton MR spectrum originate from the methylene protons (1.3 ppm) and methyl protons (0.9 ppm) of lipids. In normal healthy brain, these peaks are absent, although inappropriate volume selection may result in contamination of the spectrum with lipid signals from tissue close to the skull. Lipid signals in pathology are generally associated with necrosis such as in high-grade brain tumors or metastases. In addition, lipid signals have been observed in brain MR spectra of patients with multiple sclerosis (Wolinsky et al. 1990), Niemann-Pick disease type C (a lipid storage disorder; Sylvain et al. 1994), and patients suffering from peroxisomal disorders affecting lipid metabolism such as Zellweger syndrome and Refsum's disease (Cecil 2006). Lipid signals of varying intensity including very high peaks have been observed in white matter of patients with Sjögren–Larsson syndrome (Fig. 7), which is caused by a defect in fatty acid aldehyde dehydrogenase (Willemsen et al. 2004). In contrast, no increased lipid signal is present in the spectra of gray matter in these patients. A metabolite map of the lipid signal shows that this metabolite has its highest concentration around the frontal and occipital trigones of the ventricles (Fig. 7).

Further examples of intense resonances of otherwise absent metabolites in the brain MR spectrum of patients with metabolic defects include the occurrence of high resonances of the polyols arabinitol and ribitol (~3.75 ppm) in ribose-5-phosphate isomerase deficiency (Van der Knaap et al. 1999) and the presence of a prominent succinic acid resonance (2.39 ppm) in succinic acid dehydrogenase or complex II deficiency (Brockmann et al. 2002).

The signals of most other metabolites are smaller than those mentioned so far, often due to splitting of the signals into multiplets. In normal brain MR spectra, multiplet signals of glutamate (Glu) and glutamine (Gln) appear in the spectral regions 2.2–2.4 ppm and 3.6–3.8 ppm. In particular at 1.5 T, the resonances of these two metabolites are difficult to separate, and therefore the sum of these is often referred to as Glx. Glutamate is an important neurotransmitter, but glutamine seems to respond to disease mostly with increased cerebral concentration, for example, in Reyes syndrome, hepatic encephalopathy, and hypoxic encephalopathy (Ross and Blüml 2001). Some examples of increases in small MRS signals in inborn errors of metabolism are the signal increases of 3-hydroxy isovaleric acid (1.28 ppm) in 3-methylglutaconic aciduria type I (Engelke et al. 2006), of phenylalanine (7.3–7.4 ppm) in phenylketonuria (Pietz et al. 2003), and of the neurotransmitter γ-aminobutyric acid (GABA; 1.8–2.3 ppm and
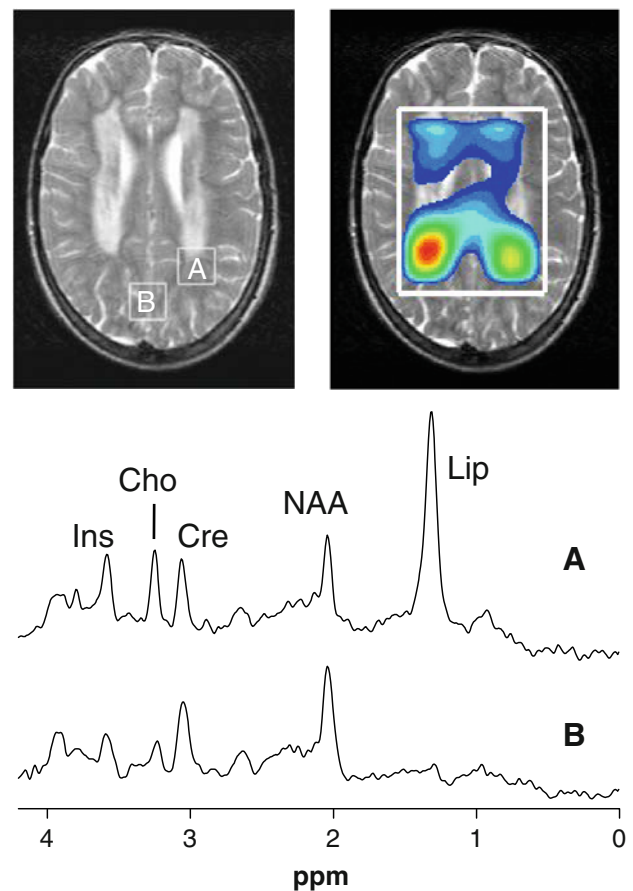

Fig. 7 MR spectra obtained at 3T (PRESS, TE/TR = 20/5,000 ms) from white (**a**) and gray matter (**b**) of a patient with Sjögren–Larsson syndrome. The spectrum of white matter clearly shows the presence of an intense lipid signal, caused by a defect in the enzyme fatty aldehyde dehydrogenase, while this resonance is absent in the spectrum of gray matter. In addition, the white-matter spectrum shows slightly increased signals of choline, creatine, and myo-inositol, associated with myelin abnormalities. The metabolite map of the lipid (*top right*) depicts its distribution with the highest intensities in the periventricular regions around the posterior and frontal trigones of the ventricles

2.9–3.1 ppm) in 4-hydroxybutyric aciduria or succinic semialdehyde dehydrogenase deficiency (Novotny et al. 2003). It should be noted that the increase in the very small signals of GABA can only be demonstrated by a special MRS editing technique.

For identification of metabolic disorders, ^{1}H MRS of the brain is predominantly used, although other parts of the body such as muscle can also be investigated or other nuclei may be used. For example, ^{31}P MRS can be used to study disturbed high-energy phosphate metabolism (Argov et al. 2000), and ^{13}C MRS has been applied to uncover hitherto unknown disorders of NAA synthesis, glutamate neurotransmission, Krebs-cycle, and glycolysis (Ross et al. 2003; Blüml et al. 2001). In addition, several body fluids such as urine, plasma, and cerebral spinal fluid of patients

suspected of an inborn error of metabolism may be analyzed in vitro by high-resolution NMR (Moolenaar et al. 2003), which offers the advantage of much higher sensitivity and resolution. For an extensive overview of in vitro ^{1}H-NMR spectroscopy of body fluids together with some examples of in vivo ^{1}H MRS in inborn errors of metabolism, the reader is referred to a recent handbook on this subject (Engelke et al. 2007).
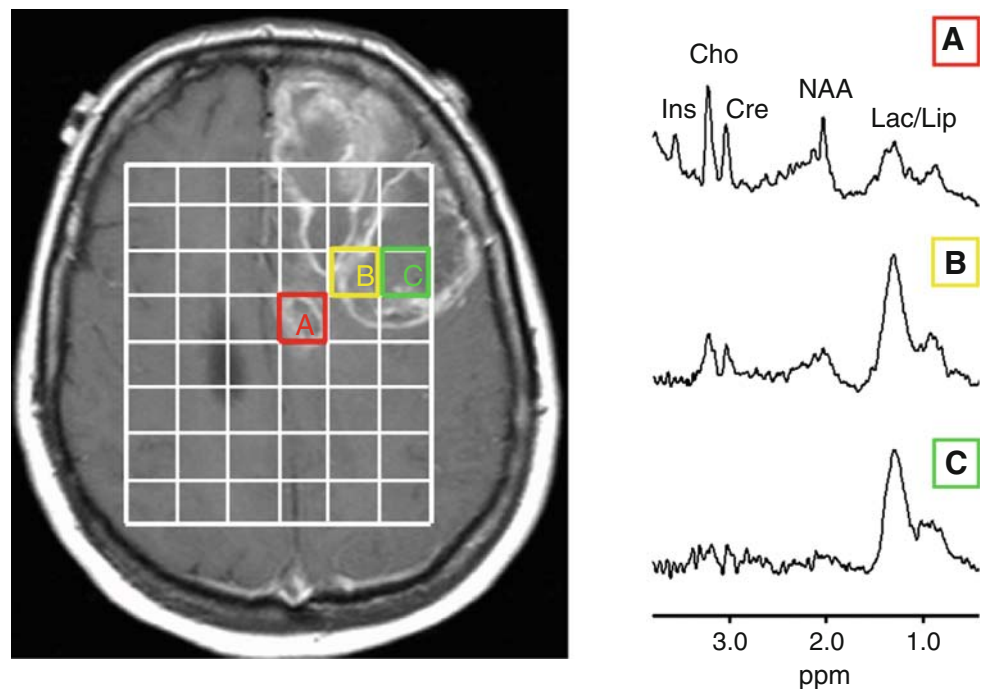
Brain tumors

Oncology is another field in which MRS is more and more used both in a research setting and in the clinic. As in tumor growth metabolism changes dramatically, MRS can add valuable information to that obtained by conventional radiological techniques such as MRI. Generally, the resonance of total choline (3.2 ppm) increases in tumors. This elevation is mainly caused by an increased rate of membrane synthesis in cancer cells, and the increase in the Cho signal is mostly caused by an increase in phosphocholine and glycerophosphoryl choline, compounds involved in membrane synthesis and degradation. In oncology, MRS is mostly used to diagnose and investigate tumors in brain (Nelson et al. 2002; Howe et al. 2003), prostate (Heerschap et al. 1997), and breast (Bolan et al. 2005); the application in brain will be discussed in more detail below. Most brain tumors belong to the group of gliomas that originate from the glial cells in the brain. Gliomas can be classified by cell type (e.g., originating from oligodendrocytes or from astrocytes), by grade (low grade is relatively benign and

high grade is very malignant), and by location. An example of a tumor that does not originate from glial cells is a meningioma, which originates from the meninges. MRS may play a role in diagnosis, biopsy guidance to reduce misdiagnosis or sometimes even replacing a biopsy, planning of surgery or radiotherapy, and monitoring of treatment response or tumor recurrence.

As mentioned above, brain tumors generally show an increase in the Cho signal, and the Cho level is believed to correlate directly with proliferative potential and malignancy (Herminghaus et al. 2002). Therefore, an increase in the total choline signal is often used in the diagnosis of a brain tumor. However, care should be taken as an elevated Cho signal may also appear in other pathologies, such as inflammation, stroke, radiation necrosis, reactive gliosis, and multiple sclerosis. In addition, the correlation between malignancy and total choline signal is not straightforward as high-grade gliomas such as glioblastoma multiforme may be very heterogeneous containing regions with necrosis resulting mainly in lipid signals and other regions with highly proliferating cells with high choline signals (Fig. 8).

In contrast to Cho, the signal of the neuronal marker NAA is generally reduced in brain tumors, due to the fact that most brain tumors are non-neuronal in origin. Also a reduced NAA is not specific for brain tumors but may occur in other pathologies such as stroke and multiple sclerosis. As the signal intensity changes in Cho and NAA appear in opposite directions in brain tumors, changes in the ratio of these two (the choline-NAA index) are often

Fig. 8a–c On the *left*, an MR image of a patient with a glioblastoma multiforme showing regions with enhanced signal intensity after contrast administration, which is indicative of a defective blood–brain barrier as is often present in high-grade brain tumors. An MRSI grid is superimposed on the MR image with three voxel positions labeled *A–C*, for which the corresponding spectra (acquired with TE = 20 ms) are presented. The variety in the spectral patterns is indicative of the tissue heterogeneity inside the brain tumor, from viable tumor tissue with a high choline signal (**a**) to necrotic tissue represented by only a lipid signal (**c**)

used to depict regions of abnormality in MRSI spectra of brain tumors (Nelson et al. 2002; Fig. 4c).

The signal of creatine is often reduced in brain tumors as a result of altered energy metabolism. Only in gliomatosis cerebri, an uncommon type of glioma, might the creatine signal be increased (Galanaud et al. 2003). Metabolites that are useful in the characterization of brain tumors include Ins and Glx. Myo-inositol is high in low-grade gliomas and decreases when the tumor grade increases (Howe et al. 2003). The signal intensity of glutamine and glutamate (Glx) can be used to distinguish between oligodendroglioma (high Glx) and astrocytoma (lower Glx) (Rijpkema et al. 2003). Glx is also high in meningioma, of which the spectra may also show signals of alanine, which is very specific for this tumor type (Howe et al. 2003). As mentioned before, lactate is caused by anaerobic metabolism, and its signal often appears in spectra of brain tumors (see Fig. 4c). However, the intensity of the lactate signals seems not to correlate with tumor malignancy (Kugel et al. 1992). Finally, signals of lipids and macromolecules are characteristic of necrotic regions in very malignant tumors and metastases (Howe et al. 2003; Opstad et al. 2004). Increases in signals of lactate and lipids in time may therefore indicate the conversion of a low-grade tumor into a more malignant one.

MRS of brain tumors may consist of single-voxel MRS, in which often one voxel is located in the lesion and another at a similar position in the contra-lateral hemisphere of the brain, allowing the spectral patterns of both the lesion and healthy tissue to be compared. As brain tumors are often heterogeneous, multivoxel MRSI can be very helpful to assess the spatial distribution of the most aggressive part of the tumor (Fig. 8). In addition, high-grade tumors often infiltrate surrounding tissue; this only becomes visible by MRSI showing spectra with abnormal patterns outside the lesion with increased signal intensity in contrast-enhanced MRI. Therefore, MRSI may also help to distinguish between a high-grade glioma and a metastasis, as the glioma generally shows infiltrations and a metastasis is spatially restricted. In addition, the ratio between lipid methylene signal intensity at 1.3 ppm and lipid methyl signal intensity at 0.9 ppm has been shown to be higher in metastases than in high-grade gliomas (Opstad et al. 2004).

In Fig. 9a an example is shown of an MR spectrum with a high lipid signal obtained from a brain lesion of a patient who had been treated by gamma-knife radiosurgery to remove a metastasis caused by breast cancer. The lesion could be a new metastasis or radiation necrosis due to the radiation therapy. Based on MRI, these two possibilities
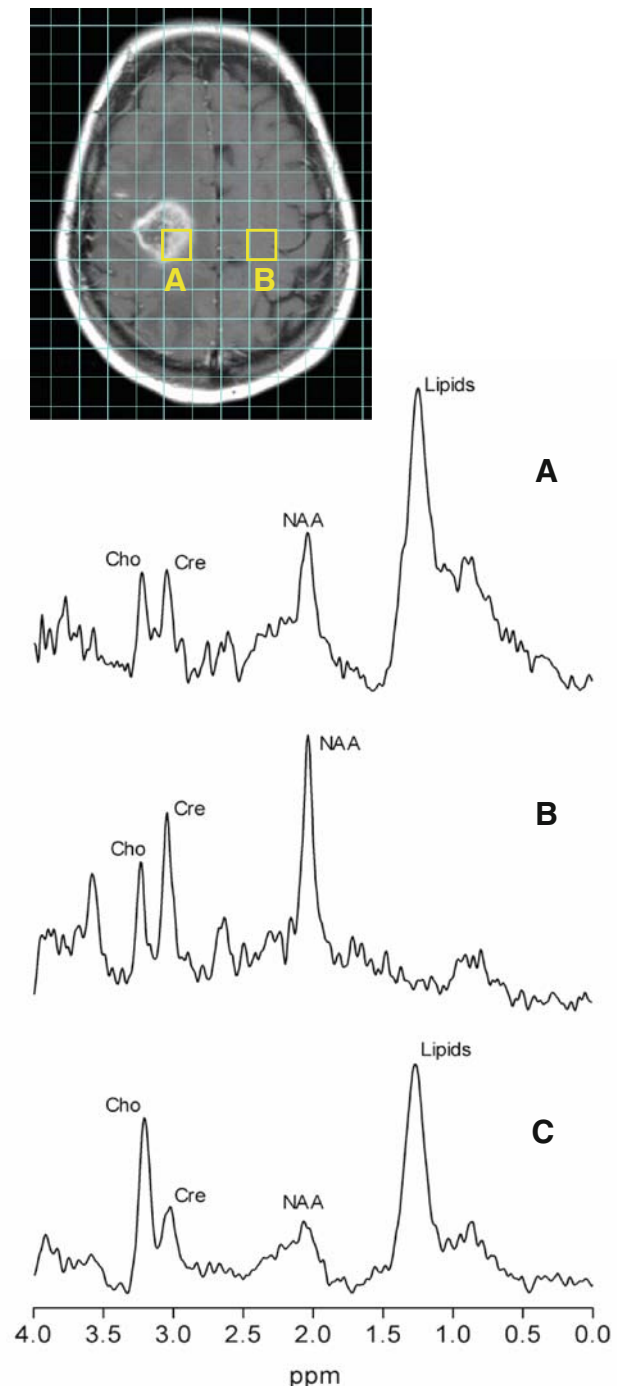

Fig. 9a–c MR image with enhanced signal intensity after contrast administration, which could be caused by the presence of a metastasis or radiation necrosis, together with an MRSI grid (TE = 20 ms). **a** Spectrum of voxel in enhancing region with rather normal intensities of the major brain metabolites creatine, choline, and NAA and a large lipid resonance. **b** Spectrum of contralateral voxel in healthy tissue showing a normal pattern of brain metabolite signals. **c** Spectrum of a metastasis obtained from another patient. Based upon the pattern of spectrum **a**, the diagnosis of radiation necrosis could be made

could not be differentiated, but as the MR spectrum showed rather normal intensities of Cho and NAA in combination with a high lipid signal, the diagnosis of radiation necrosis could be made.

Although ^{1}H MRS provides valuable information on brain tumors, clinicians are not routinely using this information, mainly because they have no or limited access to the analysis software and they have no experience in interpreting the MR spectra. Within the multicenter project INTERPRET, software has been developed based on pattern recognition techniques to help clinicians with the differentiation of brain tumors using information from ^{1}H MR spectra, mainly obtained from single voxels located in the tumor (Tate et al. 2006). In the subsequent multicenter project eTUMOUR (http://www.etumour.net/), the work by the INTERPRET consortium has been further elaborated. In this most recent project, not only data from SVS spectra are taken into account, but also multivoxel MRSI data together with information obtained from high-resolution magic-angle spinning NMR spectra of biopsy material and from analyses by DNA microarrays. Such multicenter initiatives will certainly contribute to a more general implementation of MRS in the clinic.

In addition to ^{1}H MRS, ^{31}P and ^{13}C MRS can also be used to investigate brain tumors. ^{31}P MRS has already been used to investigate pH or ratios of phosphodiesters and phosphomonoesters in brain tumors in vitro and in vivo for a long time (Stubbs et al. 1995; Maintz et al. 2002). Recent technical developments to increase ^{31}P MRS sensitivity based upon polarization transfer from ^{1}H to ^{31}P (Klomp et al. 2008b) together with the availability of more MR systems with higher field strength may result in a more frequent use of ^{31}P MRS to follow tumor treatment response. ^{13}C MRS has been used for several in vitro studies and in vivo investigations on animal models. In addition, increased dynamic lactate production has recently been shown in vivo in a high-grade brain tumor by ^{13}C MRS using polarization transfer (Klomp et al. 2008a) during infusion with ^{13}C-labeled glucose in a patient (Wijnen et al. 2008). Further, ^{13}C MRS can play an important role in the detection of hyperpolarized compounds. By injection of hyperpolarized ^{13}C-labeled compounds, a technique only recently introduced in in vivo MRS, the MR signal can be enhanced on the order of 10,000-fold (Ardenkjaer-Larsen et al. 2003). This technique has presently—at the time of writing—only been used in preclinical studies in animals and not (yet) in humans, but human applications are expected to be performed in the near future and the potential in cancer research and biomedicine in general is very promising.

Conclusions

It has been shown that NMR is not limited to applications in chemistry, but that MRS is also a valuable tool in the clinic. With the present availability of MR scanners with sufficiently high field strength such as 3T in combination with optimized pulse sequences and RF coils, the initial limited sensitivity of in vivo MRS has been much improved. This, in combination with the unique metabolic information provided by MRS, ensures that this technique will be used more and more routinely in the clinic in the future.

References

Ardenkjaer-Larsen JH, Fridlund B, Gram A, Hansson G, Hansson L, Lerche MH, Servin R, Thaning M, Golman K (2003) Increase in signal-to-noise ratio of >10,000 times in liquid-state NMR. Proc Natl Acad Sci USA 100:10158–10163

Argov Z, Löfberg M, Arnold DL (2000) Insights into muscle diseases gained by phosphorus magnetic resonance spectroscopy. Muscle Nerve 23:1316–1334

Baslow MH (2002) Evidence supporting a role for N-acetyl-L-aspartate as a molecular water pump in myelinated neurons in the central nervous system. An analytical review. Neurochem Int 40:295–300

Blüml S, Moreno A, Hwang JH, Ross BD (2001) 1-(13)C glucose magnetic resonance spectroscopy of pediatric and adult brain disorders. NMR Biomed 14:19–32

Bolan PJ, Nelson MT, Yee D, Garwood M (2005) Imaging in breast cancer: magnetic resonance spectroscopy. Breast Cancer Res 7:149–152

Bottomley PA (1987) Spatial localization in NMR-spectroscopy in vivo. Ann N Y Acad Sci 508:333–348

Brockmann K, Bjornstad A, Dechent P, Korenke CG, Smeitink J, Trijbels JM, Athanassopoulos S, Villagran R, Skjeldal OH, Wilichowski E, Frahm J, Hanefeld F (2002) Succinate in dystrophic white matter: a proton magnetic resonance spectroscopy finding characteristic for complex II deficiency. Ann Neurol 52:38–46

Brown TR (1992) Practical applications of chemical shift imaging. NMR Biomed 5:238–243

Brown TR, Kincaid BM, Ugurbil K (1982) NMR chemical shift imaging in three dimensions. Proc Natl Acad Sci USA 79:3523–3526

Cavassila S, Deval S, Huegen C, van Ormondt D, Graveron-Demilly D (2001) Cramér-Rao bounds: an evaluation tool for quantitation. NMR Biomed 14:278–283

Cecil KM (2006) MR spectroscopy of metabolic disorders. Neuroimaging Clin N Am 16:87–116

Cecil KM, Salomons GS, Ball WS, Wong B, Chuck G, Verhoeven NM, Jakobs C, DeGrauw TJ (2001) Irreversible brain creatine deficiency with elevated serum and urine creatine: a creatine transporter defect? Ann Neurol 49:401–404

Duyn JH, Moonen CT (1993) Fast proton spectroscopic imaging of human brain using multiple spin-echoes. Magn Reson Med 30:409–414

Duyn JH, Gillen J, Sobering G, van Zijl PC, Moonen CT (1993) Multisection proton MR spectroscopic imaging of the brain. Radiology 188:277–282

Dydak U, Weiger M, Pruesmann KP, Meier D, Boesiger P (2001) Sensitivity-encoded spectroscopic imaging. Magn Reson Med 46:713–722

Engelke UF, Kremer B, Kluijtmans LA, van der Graaf M, Morava E, Loupatty FJ, Wanders RJ, Moskau D, Loss S, van den Bergh E, Wevers RA (2006) NMR spectroscopic studies on the late onset form of 3-methylglutaconic aciduria type I and other defects in leucine metabolism. NMR Biomed 19:271–278

Engelke UFH, Moolenaar SH, Hoenderop SMGC, Morava E, van der Graaf M, Heerschap A, Wevers RA (2007) Handbook of 1H-NMR spectroscopy in inborn errors of metabolism: body fluid NMR spectroscopy and in vivo MR spectroscopy. Fully revised 2nd edn. SPS Publications, Heilbronn

Frahm J, Bruhn H, Gyngell ML, Merboldt KD, Hänicke W, Sauter R (1989) Localized high-resolution proton NMR spectroscopy using stimulated echoes: initial applications to human brain in vivo. Magn Reson Med 9:79–93

Fujita H (2007) New horizons in MR technology: RF coil designs and trends. Magn Reson Med Sci 6:29–42

Galanaud D, Chinot O, Nicoli F, Confort-Gouny S, Le Fur Y, Barrie-Attarian M, Ranjeva JP, Fuentès S, Viout P, Figarella-Branger D, Cozzone PJ (2003) Use of proton magnetic resonance spectroscopy of the brain to differentiate gliomatosis cerebri from low-grade glioma. J Neurosurg 98:269–276

Gruber S, Pinker K, Riederer F, Chmelík M, Stadlbauer A, Bittsanský M, Mlynárik V, Frey R, Serles W, Bodamer O, Moser E (2008) Metabolic changes in the normal ageing brain: consistent findings from short and long echo time proton spectroscopy. Eur J Radiol 68:320–327

Haase A, Frahm J, Hanicke W, Matthaei D (1985) ^{1}H NMR chemical shift selective (CHESS) imaging. Phys Med Biol 30:341–344

Heerschap A, Jager GJ, van der Graaf M, Barentsz JO, de la Rosette JJ, Oosterhof GO, Ruijter ET, Ruijs SH (1997) In vivo proton MR spectroscopy reveals altered metabolite content in malignant prostate tissue. Anticancer Res 17:1455–1460

Heindel W, Kugel H, Roth B (1993) Noninvasive detection of increased glycine content by proton MR spectroscopy in the brains of two infants with nonketotic hyperglycinemia. Am J Neuroradiol 14:629–635

Hennig J (2008) Ultra high field MR: useful instruments or toys for the boys? MAGMA 21:1–3

Herminghaus S, Pilatus U, Möller-Hartmann W, Raab P, Lanfermann H, Schlote W, Zanella FE (2002) Increased choline levels coincide with enhanced proliferative activity of human neuroepithelial brain tumors. NMR Biomed 15:385–392

Hoult DI, Richards RE (1976) The signal-to-noise ratio of the nuclear magnetic resonance experiment. J Magn Reson 24:71–85

Howe FA, Barton SJ, Cudlip SA, Stubbs M, Saunders DE, Murphy M, Wilkins P, Opstad KS, Doyle VL, McLean MA, Bell BA, Griffiths JR (2003) Metabolic profiles of human brain tumors

using quantitative in vivo 1H magnetic resonance spectroscopy. Magn Reson Med 49:223–232

in 't Zandt H, van der Graaf M, Heerschap A (2001) Common processing of in vivo MR spectra. NMR Biomed 14:224–232

Item CB, Stöckler-Ipsiroglu S, Stromberger C, Mühl A, Alessandrì MG, Bianchi MC, Tosetti M, Fornai F, Cioni G (2001) Arginine:glycine amidinotransferase deficiency: the third inborn error of creatine metabolism in humans. Am J Hum Genet 69:1127–1133

Janson CG, McPhee SW, Francis J, Shera D, Assadi M, Freese A, Hurh P, Haselgrove J, Wang DJ, Bilaniuk L, Leone P (2006) Natural history of Canavan disease revealed by proton magnetic resonance spectroscopy (1H-MRS) and diffusion-weighted MRI. Neuropediatrics 37:209–221

Klomp DW, Kentgens AP, Heerschap A (2008a) Polarization transfer for sensitivity-enhanced MRS using a single radio frequency transmit channel. NMR Biomed 21:444–452

Klomp DW, Wijnen JP, Scheenen TW, Heerschap A (2008b) Efficient 1H to 31P polarization transfer on a clinical 3T MR system. Magn Reson Med 60:1298–1305

Klose U (1990) In vivo proton spectroscopy in presence of eddy currents. Magn Reson Med 14:26–30

Kreis R, Ernst T, Ross BD (1993) Development of the human brain: in vivo quantification of metabolite and water content with proton magnetic resonance spectroscopy. Magn Reson Med 30:424–437

Kugel H, Heindel W, Ernestus RI, Bunke J, du Mesnil R, Friedmann G (1992) Human brain tumors: spectral patterns detected with localized H-1 MR spectroscopy. Radiology 183:701–709

Li BS, Wang H, Gonen O (2003) Metabolite ratios to assumed stable creatine level may confound the quantification of proton brain MR spectroscopy. Magn Reson Imaging 21:923–928

Maintz D, Heindel W, Kugel H, Jaeger R, Lackner KJ (2002) Phosphorus-31 MR spectroscopy of normal adult human brain and brain tumors. NMR Biomed 15:18–27

Martin E, Capone A, Schneider J, Hennig J, Thiel T (2001) Absence of N-acetylaspartate in the human brain: impact on neurospectroscopy? Ann Neurol 49:518–521

Maudsley AA, Matson GB, Hugg JW, Weiner MW (1994) Reduced phase encoding in spectroscopic imaging. Magn Reson Med 31:645–651

Michaelis T, Merboldt KD, Bruhn H, Hänicke W, Frahm J (1993) Absolute concentrations of metabolites in the adult human brain in vivo: quantification of localized proton MR spectra. Radiology 187:219–227

Moolenaar SH, Engelke UF, Wevers RA (2003) Proton nuclear magnetic resonance spectroscopy of body fluids in the field of inborn errors of metabolism. Ann Clin Biochem 40:16–24

Nelson SJ, Graves E, Pirzkall A, Li X, Antiniw Chan A, Vigneron DB, McKnight TR (2002) In vivo molecular imaging for planning radiation therapy of gliomas: an application of 1H MRSI. J Magn Reson Imaging 16:464–476

Novotny EJ Jr, Fulbright RK, Pearl PL, Gibson KM, Rothman DL (2003) Magnetic resonance spectroscopy of neurotransmitters in human brain. Ann Neurol 54(Suppl 6):S25–S31

Ogg RJ, Kingsley PB, Taylor JS (1994) WET, a T1- and B1-insensitive water suppression method for in vivo localized 1H NMR spectroscopy. J Magn Reson B 104:1–10

Opstad KS, Murphy MM, Wilkins PR, Bell BA, Griffiths JR, Howe FA (2004) Differentiation of metastases from high-grade gliomas using short echo time 1H spectroscopy. J Magn Reson Imaging 20:187–192

Ordidge RJ, Bendall MR, Gordon RE, Connelly A (1985) Volume selection for in vivo biological spectroscopy. In: Govil G, Khetrapal CL, Saran A (eds) Magnetic resonance in biology and medicine. Tata McGraw-Hill, New Delhi, pp 387–397

Pietz J, Lutz T, Zwygart K, Hoffmann GF, Ebinger F, Boesch C, Kreis R (2003) Phenylalanine can be detected in brain tissue of healthy subjects by 1H magnetic resonance spectroscopy. J Inherit Metab Dis 26:683–692

Posse S, DeCarli C, Le Bihan D (1994) Three-dimensional echo-planar MR spectroscopic imaging at short echo times in the human brain. Radiology 192:733–738

Pouwels PJ, Frahm J (1998) Regional metabolite concentrations in human brain as determined by quantitative localized proton MRS. Magn Reson Med 39:53–60

Pouwels PJ, Brockmann K, Kruse B, Wilken B, Wick M, Hanefeld F, Frahm J (1999) Regional age dependence of human brain metabolites from infancy to adulthood as detected by quantitative localized proton MRS. Pediatr Res 46:474–485

Provencher SW (1993) Estimation of metabolite concentrations from localized in vivo proton NMR spectra. Magn Reson Med 30:672–679

Rijpkema M, Schuuring J, van der Meulen Y, van der Graaf M, Bernsen H, Boerman R, van der Kogel A, Heerschap A (2003) Characterization of oligodendrogliomas using short echo time 1H MR spectroscopic imaging. NMR Biomed 16:12–18

Ross B, Blüml S (2001) Magnetic resonance spectroscopy of the human brain. Anat Rec 265:54–84

Ross B, Lin A, Harris K, Bhattacharya P, Schweinsburg B (2003) Clinical experience with 13C MRS in vivo. NMR Biomed 16:358–369

Scheenen TW, Klomp DW, Wijnen JP, Heerschap A (2008) Short echo time 1H-MRSI of the human brain at 3T with minimal chemical shift displacement errors using adiabatic refocusing pulses. Magn Reson Med 59:1–6

Schmidt CW (2004) Metabolomics: what's happening downstream of DNA. Environ Health Perspect 112:A410–A415

Schulte RF, Le Roux P, Vogel MW, Koenig H (2008) Design of phase-modulated broadband refocusing pulses. J Magn Reson 190:271–279

Skoch A, Jiru F, Bunke J (2008) Spectroscopic imaging: basic principles. Eur J Radiol 67:230–239

Soher BJ, Hurd RE, Sailasuta N, Barker PB (1996) Quantitation of automated single-voxel proton MRS using cerebral water as an internal reference. Magn Reson Med 36:335–339

Stöckler S, Holzbach U, Hanefeld F, Marquardt I, Helms G, Requart M, Hänicke W, Frahm J (1994) Creatine deficiency in the brain: a new, treatable inborn error of metabolism. Pediatr Res 36:409–413

Stöckler S, Hanefeld F, Frahm J (1996) Creatine replacement therapy in guanidinoacetate methyltransferase deficiency, a novel inborn error of metabolism. Lancet 348:789–790

Stubbs M, Veech RL, Griffiths JR (1995) Tumor metabolism: the lessons of magnetic resonance spectroscopy. Adv Enzyme Regul 35:101–115

Sylvain M, Arnold DL, Scriver CR, Schreiber R, Shevell MI (1994) Magnetic resonance spectroscopy in Niemann-Pick disease type C: correlation with diagnosis and clinical response to cholestyramine and lovastatin. Pediatr Neurol 10:228–232

Tate AR, Underwood J, Acosta DM, Julià-Sapé M, Majós C, Moreno-Torres A, Howe FA, van der Graaf M, Lefournier V, Murphy MM, Loosemore A, Ladroue C, Wesseling P, Luc Bosson J, Cabañas ME, Simonetti AW, Gajewicz W, Calvar J, Capdevila A, Wilkins PR, Bell BA, Rémy C, Heerschap A, Watson D, Griffiths JR, Arús C (2006) Development of a decision support system for diagnosis and grading of brain tumors using in vivo magnetic resonance single voxel spectra. NMR Biomed 19:411–434

Van der Knaap MS, Wevers RA, Struys EA, Verhoeven NM, Pouwels PJ, Engelke UF, Feikema W, Valk J, Jakobs C (1999) Leukoencephalopathy associated with a disturbance in the metabolism of polyols. Ann Neurol 46:925–928

Varho T, Komu M, Sonninen P, Holopainen I, Nyman S, Manner T, Sillanpää M, Aula P, Lundbom N (1999) A new metabolite contributing to N-acetyl signal in 1H MRS of the brain in Salla disease. Neurology 52:1668–1672

Wijnen JP, Klomp DW, Idema AJ, de Galan BE, Heerschap A (2008) Lactate production in human brain tumor; detection by 13C MRS at 3T. Abstract. Proc Intl Soc Mag Reson Med 16:2815

Willemsen MA, Van Der Graaf M, Van Der Knaap MS, Heerschap A, Van Domburg PH, Gabreëls FJ, Rotteveel JJ (2004) MR imaging and proton MR spectroscopic studies in Sjögren–Larsson syndrome: characterization of the leukoencephalopathy. Am J Neuroradiol 25:649–657

Wolinsky JS, Narayana PA, Fenstermacher MJ (1990) Proton magnetic resonance spectroscopy in multiple sclerosis. Neurology 40:1764–1769

Yue Q, Isobe T, Shibata Y, Anno I, Kawamura H, Yamamoto Y, Takano S, Matsumura A (2008) New observations concerning the interpretation of magnetic resonance spectroscopy of meningioma. Eur Radiol 18:2901–2911